Title

Ventral medullary control of rapid eye movement sleep and atonia.

Authors

Chen, Michael C
Vetrivelan, Ramalingam
Guo, Chun-Ni
et al.

Publication Date

2017-04-01

DOI

10.1016/j.expneurol.2017.01.002

Peer reviewed

Published in final edited form as:

Exp Neurol. 2017 April ; 290: 53–62. doi:10.1016/j.expneurol.2017.01.002.

Ventral medullary control of rapid eye movement sleep and atonia☆

Michael C. Chen[a,1], **Ramalingam Vetrivelan**[a,1], **Chun-Ni Guo**[c], **Catie Chang**[b], **Patrick M. Fuller**[a,2], and **Jun Lu**[a,*,1,2]

[a]Beth Israel Deaconess Medical Center and Harvard Medical School, Department of Neurology, Division of Sleep Medicine, Boston, MA 02115, USA

[b]Advanced Magnetic Resonance Imaging Section, Laboratory of Functional and Molecular Imaging, National Institute of Neurological Disorders and Stroke, National Institutes of Health, Bethesda, MD 20892, USA

[c]Department of Neurology, Shanghai First People's Hospital Shanghai Jiaotong University, Shanghai, China

Abstract

Discrete populations of neurons at multiple levels of the brainstem control rapid eye movement (REM) sleep and the accompanying loss of postural muscle tone, or atonia. The specific contributions of these brainstem cell populations to REM sleep control remains incompletely understood. Here we show in rats that viral vector-based lesions of the ventromedial medulla at a level rostral to the inferior olive (pSOM) produced violent myoclonic twitches and abnormal electromyographic spikes, but not complete loss of tonic atonia, during REM sleep. Motor tone during non-REM (NREM) sleep was unaffected in these same animals. Acute chemogenetic activation of pSOM neurons in rats robustly and selectively suppressed REM sleep but not NREM sleep. Similar lesions targeting the more rostral ventromedial medulla (RVM) did not affect sleep or atonia, while chemogenetic stimulation of the RVM produced wakefulness and reduced sleep. Finally, selective activation of vesicular GABA transporter (VGAT) pSOM neurons in mice produced complete suppression of REM sleep whereas their loss increased EMG spikes during REM sleep. These results reveal a key contribution of the pSOM and specifically the VGAT+ neurons in this region in REM sleep and motor control.

Keywords

REM arousal; GABA; VGAT; DREADD; AAV

☆The authors declare no competing financial interests.

*Corresponding author at: Center for Life Sciences 717, 3 Blackfan Circle, Boston, MA 02115, USA. jlu@bidmc.harvard.edu (J. Lu).

[1]These authors contributed equally to this work.

[2]Contributing equally senior authors.

Supplementary data to this article can be found online at http://dx.doi.org/10.1016/j.expneurol.2017.01.002.

1. Introduction

A network of brainstem and spinal cord premotor and motor neurons produce a loss of muscle tone, termed atonia, during rapid eye movement (REM) sleep. The central generators of atonia are located in the dorsal pons and ventral medulla (Lai and Siegel, 1997; Hajnik et al., 2000). Within the dorsolateral pons, REM-active glutamatergic cells in the sublaterodorsal nucleus (SLD) in rats and mice project directly to the ventral horn of the spinal cord and mediate REM sleep atonia (Lu et al., 2006; Krenzer et al., 2011). The ventral medulla, on the other hand, contains more diffuse cell populations that regulate atonia through direct projections to the spinal cord and other motoneuron populations (Chase et al., 1984; Holmes and Jones, 1994). Ultimately, it is the hyperpolarization of motoneurons during REM sleep (Nakamura et al., 1978) that produces atonia, with the inhibitory drive deriving from glycinergic inhibitory post-synaptic potentials (Chase et al., 1989; Chase and Morales, 1990) at the level of the spinal cord ventral horn, although some motor systems may have alternative inhibitory mechanisms (Morrison et al., 2003; Brooks and Peever, 2008). How this brainstem-spinal cord network, in particular the different levels of the medulla, contributes to REM sleep atonia remains incompletely understood.

Reticulospinal neurons in the rostral and caudal medulla are predominantly glycine-GABAergic and glutamatergic, respectively, although both neuronal subtypes are found across all levels of the medulla (Hossaini et al., 2012). Consistent with this subtype distribution, genetic disruption of glutamatergic neurotransmission within the caudally-situated supraolivary (SOM) medulla produced exaggerated muscle twitches during REM sleep whereas disruption of GABA/glycinergic neurotransmission produced only minor effects with fewer muscle twitches (Vetrivelan et al., 2009). Another study, emphasizing a more caudal level of the medulla, demonstrated a role for medullary GABA/glycine, but not glutamate, in atonia control (Lai et al., 2010).

Given that medullary areas rostral to the SOM level contain a higher proportion of spinally-projecting GABA/glycine cells (Hossaini et al., 2012), we hypothesized that this level, which we term the pre-supraolivary medulla (pSOM), contributes to REM sleep atonia using GABA/glycine. We tested this hypothesis by lesioning, inhibiting or activating the pSOM and measuring EMG activity during REM sleep in rats. Using a separate cohort of rats we lesioned and inhibited the medullary region immediately rostral to the pSOM, the RVM, which also contains GABA/glycine neurons that project to the spinal cord, but receives a smaller input from the SLD. Finally, to define the specific role of GABAergic/glycinergic medullary neurons in REM sleep and atonia control, we used a ligand-driven system and Vgat-IRES-cre mice to acutely activate and genetically ablate pSOM neurons.

2. Results

2.1. Effects of pSOM and RVM lesions using DTA

Co-infusion of AAV-DTA and AAV-cre were used to produce cell-body specific lesions of the RVM (n = 4) and pSOM (n = 5) (Fig. 1). Both the RVM (Fig. 1A) and pSOM (Fig. 1B) levels showed widespread loss of neurons in the medial portion of the medulla at the RVM and pSOM levels compared to control animals, which were injected with saline in the pSOM

(n = 4) (Fig. 1C–D). High magnification images (Fig. 1E–F) showed no Nissl-stained cells remaining within the boundaries of the lesions (left panels) compared to saline injections (right panels). At least 3 weeks post-injection, we recorded 24 h of sleep/wake activity using implanted EEG and EMG from lesioned animals. We compared these sleep recordings with 24 h sleep/wake recordings from control animals, and cell-body lesions of neither the RVM nor the pSOM significantly changed overall wakefulness (46.17 ± 2.31% of 24 h recording in controls, 44.73 ± 2.77% in RVM lesioned animals, 48.13 ± 3.04 in pSOM lesioned animals), NREM sleep (46.54 ± 2.60% in controls, 47.1 ± 2.17% in RVM lesioned animals, 45.55 ± 2.83% in pSOM lesioned animals) or REM sleep (7.10 ± 0.74 in controls, 8.17 ± 1.4% in RVM lesioned animals, 6.31 ± 1.36% in pSOM lesioned animals). There were no significant differences between control, pSOM, or RVM lesion animals in the average duration of wake bouts [$F(2,10) = 1.604$] NREM sleep bouts, [$F(2,10) = 0.176$], or REM sleep bouts, [$F(2,1) = 0.083$, $p > 0.05$]. There were also no significant difference in the number of wake bouts, [$F(2,10) = 0.558$], NREM bouts, [$F(2,10) = 0.532$], or REM bouts, [$F(2,1) = 0.008$, $p > 0.05$]. Examining the FFT power frequency during NREM sleep also revealed no overall differences in delta, theta, alpha, beta, or gamma bands. Collectively, lesions to the pSOM or RVM did not affect overall sleep wake time, or the duration or numbers of sleep bouts.

EMG and video recordings during NREM sleep and wakefulness in both RVM and pSOM lesioned animals were unremarkable, but EMG recordings during REM sleep in pSOM lesioned, but not RVM lesioned animals, showed high-amplitude phasic activity (Fig. 2A–B). Accompanying the EMG phasic spikes in pSOM lesioned animals during REM sleep, we observed violent myoclonic twitches during REM sleep in pSOM lesioned, but not in control or RVM lesioned animals. Most rats showed some twitches during REM sleep, but pSOM lesioned animals often twitched violently in rapid succession or with enough force to throw their midsections in the air. We used frame-by-frame analysis of video taken during REM sleep to capture these phasic movements (Fig. 2C–D). This video analysis revealed different types of REM sleep movements related to different REM sleep EMG phenomena. Movements were always accompanied by EMG phenomena, but some EMG spikes did not correspond with visible movement. Fig. 2C shows the color-coded movement of a pSOM-lesioned animal time-locked with the EMG. Visible movement, show in red, occurred at the end of the 6 s period shown, despite EMG signal changes throughout the period. In contrast, Fig. 2D shows another 6 s period of REM sleep in another pSOM lesioned animal. Here, a single EMG signal abnormality was visible, and the color-coded video screenshots of the animal's movement, time-locked with the EMG, showed whole-body movement before (blue), during (green), and after (yellow and orange) the EMG signal abnormality (Fig. 2D; Movie S1). In general, the movements during REM sleep in pSOM lesioned animals were violent but simple. The typical behavior was a straight, up-and-down twitch, without coordinated limb movements. These movements lifted the entire body with enough force to shake the animal's cage and the video camera outside the cage. Surprisingly, despite the violence and whole-body involvement of these behaviors, pSOM lesioned animals very rarely woke up following these movements. Animals continued through REM sleep unperturbed, and pSOM lesioned animals did not show a significant reduction in total REM sleep time, despite these REM sleep movements throughout the 24 h recording period.

We examined the EMG signal during NREM and REM sleep to test for the integrity of atonia following pSOM and RVM lesions. Because the absolute value of the EMG varied from animal to animal, we tested the ratio of the average EMG signal in an epoch of wakefulness, and NREM and REM sleep. ANOVA tests of these ratios showed no significant differences between control, RVM lesion, or pSOM lesion groups in wake/NREM sleep EMG ratio, [$F(2,10) = 2.12$, $p > 0.05$], wake/REM sleep EMG ratio, [$F(2,10) = 2.11$, $p > 0.05$], or in REM/NREM sleep EMG ratio, [$F(2,10) = 0.59$, $p > 0.05$]. These latter ratios were 0.82 in controls, 0.82 in pSOM lesions, and 0.92 in RVM lesions. In each case, the average integral of the EMG during a REM sleep epoch was less than during a NREM sleep epoch, consistent with the decrease in absolute EMG amplitude during REM sleep atonia. Because the average integral of the EMG may not capture brief but high-amplitude changes in the EMG, we next calculated the absolute maximum of the EMG signal, averaged across all wake, NREM sleep, and REM sleep epochs. Across control, RVM lesion, and pSOM lesion groups, there were no group differences in the wake/NREM EMG maximum ratio [$F(2,10) = 1.22$] or in the wake/REM EMG maximum ratio [$F(2,10) = 3.50$, both $p > 0.05$]. However, in examining the ratio of the absolute maximum of the EMG in REM/NREM, we found a significant difference in the groups [$F(2,10) = 6.71$, $p = 0.01$]. Post-hoc *t*-tests showed no difference between control (0.91 ratio) and RVM lesion groups (1.00 ratio) in this REM/NREM max EMG ratio, [$t = 0.45$]. However, the ratio in pSOM lesion animals (1.55 ratio) was significantly greater than both controls [$t = 3.35$] and RVM lesion groups [$t = 2.88$, $p < 0.05$]. This ratio indicates that the average REM sleep epoch in pSOM lesioned animals had an absolute maximum EMG 1.55 times higher than the average NREM sleep epoch.

This difference was likely driven by brief, high-amplitude EMG “spikes.” To quantify these phasic bursts, we marked EMG spikes that were at least twice the height (voltage) of the tonic REM sleep EMG. Compared with control animals, pSOM lesioned animals had significantly greater spikes per 10-second REM epoch (mean 3.80 spikes/epoch) compared to control animals (0.17 spikes/epoch) [$t(12) = 2.50$, $p = 0.028$]. pSOM lesioned animals also had significantly greater percentage of 10-second REM epochs with spikes (33.95%) compared to control animals (8.48%) [$t(12) = 3.21$, $p = 0.008$] (Fig. 2F). No significant increase in either the number of spikes/REM epoch or the percentage of REM epochs with spikes was observed in RVM lesioned animals. Unlike lesions of the SLD (Lu et al., 2006), we did not observe any coordinated, complex behavior, such as walking or running. We also did not observe any abnormal behaviors during NREM sleep or wakefulness in pSOM or RVM lesioned animals.

2.2. Reversible excitation of the pSOM and RVM

To and reversibly activate neurons in the medial medulla, we injected a mixture of AAV-hM3Dq, and AAV-cre into the pSOM (n = 5) and RVM (n = 4). The modified excitatory muscarinic hM3Dq receptor is selectively activated by the otherwise pharmacologically inert drug clozapine-n-oxide (CNO) and enhances neuronal excitability (Alexander et al., 2009). After habituation to the recording chamber, we injected either saline, as a control, or CNO (0.2 mg/kg) to excite transduced neurons. We recorded sleep-wake behavior for 24 h after each system administration of saline or CNO. Injection of the virus mix transduced neurons

within the RVM and pSOM, respectively (Fig. 3A–B). Outlines of the area with transduced cell bodies were similar to the spatial extent of the lesions, both centered on the medial medulla (Fig. 3C–D). Activation of these neurons with CNO 4 h prior to perfusion lead to the expression and double-staining of c-Fos+, a marker of neuronal activity, in transduced neurons (Fig. 3E), although some transduced neurons did not express c-Fos. Perfusion after injection with saline resulted in almost no c-Fos expression in transduced neurons (Fig. 3F). Double-staining counts of a section at the center of the RVM injection revealed that 4% of transduced neurons expressed c-Fos after saline injection and 71.39% of transduced neurons expressed c-Fos after CNO injection. For the pSOM, 0.93% transduced neurons expressed c-Fos after saline injection and 74.30% of transduced neurons expressed c-Fos after CNO injection.

Saline injection in RVM or pSOM virus-injected animals was followed by a transient wakefulness period and an otherwise normal 24-hour amounts of wakefulness (RVM saline 44.67 ± 2.39%, pSOM saline 45.4 ± 4.78%), NREM sleep (RVM 47.72 ± 2.51%, pSOM 48.54 ± 1.86%), and REM sleep (RVM 7.6 ± 0.87%, pSOM 6.07 ± 1.72%). There were no significant effects of CNO administration in pSOM or RVM animals on the number of EMG spikes per REM epoch or in the percentage of REM epochs with an EMG spike, nor were there significant changes in the ratios of REM/NREM sleep EMG integral or absolute maximum.

Activation of the RVM with CNO resulted in a significant increase of wakefulness within the first 6 h after injection compared to saline injection [$t(5) = 4.52$, $p = 0.006$] with an commensurate decrease in REM sleep [$t(5) = 4.28$, $p = 0.008$] and NREM sleep [$t(5) = 4.45$, $p = 0.007$] (Fig. 4A–B). Although saline injection also increases wakefulness, animals usually fall back asleep within 15–30 min of injection and return to their normal sleep rhythm. With RVM activation, we observed in every animal an increase in wakefulness during the 6 h CNO-active period ranging up to 81% (Fig. 4C). Driven by this 6 h increase in wakefulness and decrease in sleep, wakefulness was significantly increased in the 24 h period after injection (increase of 52.51 ± 3.16%) [$t(5) = 4.35$, $p = 0.007$]. During this period of wakefulness, animals exhibited a normal repertoire of waking behavior: walking, eating, drinking, grooming, etc. Animals often stood for long periods without any obvious behavior but with a desynchronized, wake-like EEG. No abnormal movements, including violent twitches, were observed. There was a large degree of variability in the average wake bout duration in the 6 h after CNO, and paired *t*-tests showed no significant consistent increase [$t(5) = 2.35$] with no significant change in average NREM or REM sleep bout duration. There were, however, significant decreases in the number of NREM sleep bouts [$t(5) = 7.214$, $p = 0.002$] and REM sleep bouts [$t(5) = 4.620$, $p = 0.010$]. Interestingly, there was also a significant decrease in the average number of wake bouts [$t(5) = 7.038$, $p = 0.002$] driven by extremely long, sustained bouts of wakefulness early in the CNO period in some animals. Over 24 h, NREM sleep was significantly diminished (decrease of 41.07 ± 2.84%) [$t(5) = 4.00$, $p = 0.01$], 24 h REM sleep percentage remained unchanged (6.39 ± 1.19%) [$p > 0.05$]. Analysis of sleep across the 18 h after the 6 h CNO period yielded no significant differences in wakefulness, [$t(5) = 1.60$], NREM sleep [$t(5) = 1.67$], or REM sleep [$t(5) = 0.16$], suggesting no compensatory rebound in sleep. In the 18 h after the CNO window, there were no significant changes to either bout numbers of durations compared to

salineinjected animals. No changes to the EEG in wake or sleep after CNO were detected after FFT analysis of major frequency bands.

Within the first 6 h of pSOM activation with CNO, we observed a reduction in REM (Fig. 5A), with an 87% reduction in REM over 6 h compared to saline injected animals [$t(4) = 3.16$, $p = 0.034$] (Fig. 5B). With pSOM activation with CNO, we observed in each animal a reduction in REM sleep ranging from 73% to 100% over the first 6 h of CNO injection (Fig. 5C). In contrast to the REM suppression, there were no significant changes in NREM sleep [$t(4) = 1.24$] or wakefulness, [$t(4) = 1.87$, $p > 0.05$]. In the 18 h after REM sleep, there were no significant differences in wakefulness, NREM, or REM sleep, and across 24 h, there were no changes to amounts of these states between CNO-injected and saline injected conditions, (Fig. 4A). While pSOM activation robustly suppresses REM sleep, there does not appear to be a substantial rebound in REM sleep in the 18 h following the CNO-active period. The suppression of REM sleep in the 6 h after CNO injection was driven by a large decrease in the average number of REM bouts from saline-injected animals (~13.8 bouts) to CNO injected animals (~1.6 bouts) [$t(5) = 4.185$, $p = 0.025$]. NREM bouts were preserved and even extended, due to the absence of transitions to REM sleep. This resulted in less NREM bouts [$t(5) = 7.574$, $p = 0.005$] and longer average NREM sleep bouts [$t(5) = 4.752$, $p = 0.018$]. The average wake duration did not change in the 6 h after CNO [$t(5) = 2.341$, $p > 0.05$] and the number of wake bouts was also significantly decreased after CNO injection [$t(5) = 8.114$, $p = 0.004$] suggesting an overall consolidation of NREM sleep-wake switching in the absence of REM sleep. FFT analysis of the EEG spectra after CNO revealed no differences in the major frequency bands (delta, theta, alpha, etc.) for NREM sleep or REM sleep in those animals with sufficient residual REM sleep for analysis. CNO activation of the pSOM did not affect atonia or the EMG during REM sleep.

2.3. GABA lesion of the pSOM in Vgat-cre mice

GABA/glycine neurons at the level of the pSOM project to the ventral horn of the spinal cord and are hypothesized to be involved in REM sleep atonia (Holstege and Bongers, 1991; Fort et al., 1993; Morales et al., 1999; Stornetta and Guyenet, 1999; Boissard et al., 2002; Hossaini et al., 2012). To determine if GABA/glycine neurons at the pSOM regulate REM sleep atonia, we selectively lesioned these neurons in VGAT-cre mice using AAV-DTA ($n = 5$). Injections of AAV-DTA produced loss of VGAT+ neurons in the pSOM region (Fig. 6A–B). Compared with wildtype littermates also injected with AAV-DTA ($n = 4$), VGAT-cre mice had no significant changes in NREM or REM sleep or wakefulness, nor did these mice show EMG changes during NREM sleep. VGAT-cre mice had greater numbers of REM sleep EMG spikes (0.65 ± 0.96 spikes/epoch) compared to wildtype littermates (0.03 ± 0.01 spikes/epoch), although the number of spikes were variable in the VGAT-cre mice. Similarly, VGAT-cre mice had a greater proportion of REM sleep epochs with EMG spikes ($11.68\% \pm 11.72\%$) compared to wildtype controls ($2.81\% \pm 1.41\%$).

2.4. Reversible excitation of the pSOM in Vgat-cre mice

In rats, excitation of the pSOM results in REM sleep suppression, however it is unclear if this effect is driven by GABA/glycine neurons. To determine if REM sleep suppression found in rats were due to GABA/glycine neurons at the pSOM level, we placed targeted

injects of hM3Dq into the pSOM of five VGAT-cre mice (Fig. 7A). As in rats, activation of pSOM neurons with CNO resulted in increased c-Fos expression in most of the transduced neurons (Fig. 7B). The injection extent covered the pSOM level of the mouse medulla (Fig. 7C).

To determine if suppression of REM sleep by activation of the pSOM is driven by GABA/glycine cells, we injected CNO to excite glycine-GABAergic neurons at 10 AM, focusing on the light-period time which normally shows a high percentage of REM sleep. Consistent with activation of the pSOM in rats, activation of GABA/glycine neurons in the pSOM in mice produced a robust reduction in REM sleep lasting about 6 h (Fig. 8A). Over this 6 h period, compared to the same time period on a separate day following saline injection, we observed a significant reduction in REM sleep without changes in NREM and wake [$t(4) = 3.42$, $p = 0.027$] (Fig. 8B). As in rats, every animal experienced a reduction in REM sleep (Fig. 8C). This reduction was driven by a significant decrease in the number of REM bouts during the first 6 h after CNO administration [$t(4) = 11.83$, $p = 0.001$] but no significant changes in the number of wake or NREM sleep bouts. As in rats, there was also a significant increase in the average bout duration of NREM sleep in the 6 h after CNO [$t(4) = 4.05$, $p = 0.02$] and the duration of wake and REM sleep bouts was also unchanged after CNO injection. As in rats, there was no significant rebound in REM sleep in the following 18 h. CNO injection also did not alter the power spectra of the EEG in delta, theta, alpha, or higher frequency bands, although we note the lack of power due to absence of REM sleep following CNO injection. As with rats, CNO activation of the pSOM did not affect atonia or the EMG during REM sleep.

3. Discussion

Decades of evidence supports the role of the ventromedial medulla in REM sleep atonia control (Castillo et al., 1991; Holstege and Bongers, 1991; Fort et al., 1993; Lai and Siegel, 1997; Morales et al., 1999; Stornetta and Guyenet, 1999; Boissard et al., 2002). Previously identified cell groups like the gigantocellular ‘nucleus’ extend across multiple levels of the rostral-caudal axis of the medulla. Here we show that lesions to the pSOM, but not RVM, level of the medulla in rats produces, likely through disinhibition, muscle twitches and movement during REM sleep atonia. Lesions of the pSOM specifically resulted in myoclonic twitches during REM sleep without affecting REM sleep time or the EMG of tonic atonia, whereas lesions of the RVM did not alter either atonia or sleep time. Acute activation of the pSOM in rats using a hM3Dq receptor resulted in a profound reduction in REM sleep time. By contrast, a similar activation of the RVM produced wakefulness and decreased NREM and REM sleep in the hours after injection but has no effect on REM sleep atonia. Selective activation of GABAergic pSOM neurons in the mouse recapitulated the REM sleep suppression phenotypes of nonselective pSOM activation in the rat. These results demonstrate that GABA/glycine neurons in the pSOM, but not in the RVM, regulate REM sleep time. Consistent with these previous studies, we demonstrate the involvement of the ventromedial medulla in REM sleep atonia. Taken together with our previous study (Vetrivelan et al., 2009), the zone of inhibitory control in the medulla appears to span the pSOM and SOM levels, forming an overlapping and continuous population of mixed

neurons that regulate REM sleep and muscle twitches during REM sleep atonia and a role for GABA/glycine pSOM neurons in suppressing REM sleep.

Neurons in the medulla are key contributors to muscle tone control during REM sleep. Stimulation of cell populations at the SOM (Vetrivelan et al., 2009) and pSOM levels reduces muscle tone in decerebrate animals (Lai et al., 2010). We show here that neurons at the pSOM level are involved in control of phasic muscle twitches during REM sleep atonia. Importantly, lesions of the pSOM and SOM do not affect the EMG signal of tonic atonia but rather lead to, presumably through disinhibition, high-amplitude phasic EMG activity during REM sleep. We note that even the largest lesions of the SOM (Vetrivelan et al., 2009) or pSOM in our study do not completely abolish atonia. Our observations also indicate a lack of complex behaviors during REM sleep after pSOM lesions in rats. Both these observations contrast with the loss of tonic atonia and disinhibition of complex behaviors with lesions of the pontine SLD. Complete REM sleep atonia–suppression of both complex behaviors and phasic twitches–likely involves multiple layers of control using multiple neurotransmitters, with medullary relays synergizing with direct SLD to spinal projections (Weng et al., 2014).

The behaviors we observed with pSOM lesions, similar to those following SOM lesions, can be described as violent myoclonic twitches during REM sleep. The most typical behavior was a single ‘jumping’ twitch in which the entire body pops up and lands, which is a similar phenotype to that observed following SOM lesions. The observed behavioral/motor activation did not necessarily match the amplitude of the EMG spikes, which would be consistent with the placement of the EMG in nuchal muscles rather than in other muscle groups. Future studies using multiple EMGs may capture a broader range of EMG abnormalities during REM sleep. Remarkably, however, these aberrant motor behaviors rarely interrupted REM sleep, as REM sleep time was not reduced with pSOM lesions, nor was the REM EEG disturbed by motor behaviors. In addition, aberrant motor behaviors were not observed during NREM sleep. These myoclonic twitches may be due to increased REM sleep phasic activity, i.e., disinhibition of motor-enhancing spinal neurons targeted by medullary neurons or a decrease in REM sleep inhibitory control, i.e., absence of excitatory input to motor-suppressing spinal neurons from medullary neurons, or both. Both GABA/glycine and glutamate project to the spinal cord, particularly spinal interneurons (Drew and Rossignol, 1990; Takakusaki et al., 2001). Following specific lesions of pSOM GABA/glycine neurons by injections of AAV-DTA, VGAT-cre mice displayed greater numbers of EMG spikes during REM sleep and they had a greater proportion of REM sleep epochs with EMG spikes indicating a critical role for pSOM GABA/glycinergic neurons in REM sleep muscle atonia. Although twitches were observed consistently, REM sleep behavior was inconsistent, with some mice displaying motor behavior while others displayed only EMG twitches. These differences could be due to magnitude of GABA/glycinergic neuronal loss within the pSOM. In addition, multiple neurotransmitters systems working synergistically may also be needed to ultimately produce the strong glycinergic tone on motoneurons across the neuraxis (Chase, 2013).

Following activation of pSOM neurons in rats and GABA/glycine pSOM neurons in mice, we observed a profound suppression of REM, but not NREM, sleep. The time course of the REM sleep suppression was about 6 h in both rats and mice, which is consistent with the

previously reported window of effect of CNO (Alexander et al., 2009; Anaclet et al., 2014). Interestingly, there was no significant REM sleep rebound in the 18 h post CNO administration, although there is the possibility of a subsequent REM rebound in following days. In contrast, a recent optogenetic stimulation study found increased REM sleep after stimulating GABA neurons in the medulla (Weber et al., 2015). These results suggest the possibility of a medullary REM sleep network containing both REM-on and REM-off populations. Cell populations in the pSOM may be sufficient for REM sleep suppression, while REM sleep initiation, on the other hand, may require the coordinated activity of both medullary and pontine glutamatergic neurons, as well as other REM-regulating medullary groups (Luppi et al., 2006). Furthermore, from the current experiments, it is unclear if there is a single population of neurons that both suppresses REM sleep and regulates motor tone during REM sleep or if there are multiple populations in the area with heterogeneous projections and functions. Careful dissection of these circuits, including precise targeting of spinal-projecting neurons, will be needed to further map this medullary REM circuit.

While lesions of the RVM did not affect sleep or wake times or atonia, activation of this region with CNO produced wakefulness, which was accompanied by decreases in both NREM and REM sleep. The transduced cells appeared to be largely within the gigantocellular fields of the RVM, which is consistent with the established role of these neurons in waking behavior (Martin et al., 2010). The behaviors observed during the period of CNO-induced wakefulness resembled normal waking behavior, including normal movement, eating, etc., but it is unclear if CNO activation of the RVM produces arousal via direct activation of wake-promoting regions like the parabrachial nucleus (Fuller et al., 2011), through descending motor activation (Martin et al., 2011), or through perturbation of the balance of normal physiological functioning in the ventromedial medulla. Regardless, the RVM, unlike the pSOM, does not appear to contribute to the regulation of either REM sleep or REM sleep atonia.

For decades, the medulla was thought to be a key intermediary of REM sleep atonia. Our findings, combined with other recent studies, suggest that the medulla may play a more specific role in REM sleep atonia: the regulation of REM twitches. In contrast, loss of the glutamatergic SLD results in a dramatic loss of atonia. Taken together, these results suggest dual pathways of REM sleep atonia control: a glutamatergic SLD projection system to the medulla and spinal cord, and a medullary system of mixed neurotransmitter phenotype, with a greater role for GABA/glycinergic neurons, that specifically regulates REM phasic muscle events, e.g., twitches, via descending projections to the spinal ventral horn (Hossaini et al., 2012). In addition, a specific population of glycine-GABA neurons in this region suppresses REM sleep, possibly via ascending connections to pontine REM sleep control circuits or through recently discovered medullary REM networks (Weber et al., 2015). The co-localization of circuitry in the medulla regulating REM sleep and patterned phasic muscle activity hints at a more complex role for the medulla than blanket suppression, perhaps even an active role in facilitating sensorimotor feedback and learning during REM sleep.

4. Materials and methods

4.1. Animals

Adult male Sprague-Dawley rats (n = 22), weighing 300–325 g (Harlan), and adult male Vgat-ires-cre and wildtype control (n = 14) mice (Vong et al., 2011), weighing 24–28 g were used in this study. Rats and mice were individually housed, with ad libitum access to food and water. All animal care was in accordance with National Institutes of Health standards, and all procedures used were approved by the Beth Israel Deaconess medical Center Institutional Animal Care and Use Committee.

4.2. Animal surgery and EEG/EMG implantation

Animal surgeries and injections were performed as described previously (Anaclet et al., 2012). Briefly, rats were anesthetized with an i.p. injection of ketamine (100 mg/kg) and xylazine (10 mg/kg) (Med-Vet) and placed into a stereotaxic frame. After exposing the cranium for measurement of coordinates relative to bregma, a burr hole was made for injection. Injections were made as previously described (Fuller et al., 2011). Briefly, all injections were used using a fine glass pipette and compressed air system that slowly delivers injections using small air puffs over 5 min. After the injection, the pipette was left in place for 5 min, then retracted. For lesions in rats, we injected 120 nL of a 1:1 admixture of an adeno-associated viral (AAV) vector expressing Cre-recombinase under the cytomegalovirus promoter (Cre-AAV, serotype 10) and an AAV expressing the cytotoxic Subunit A of Diptheria Toxin (DTA) in a cre-dependent configuration (lox-DsRED-lox-DTA-AAV, serotype 10; Beth Israel Deaconess Medical Center, USA). To achieve neuronal excitation in rats, we injected 120 nL of an AAV cocktail containing AAV-Cre and modified muscarinic G protein–coupled receptor (hM3Dq) in a cre-dependent configuration (DIO-hM3Dq-mCherry, serotype 10) (Alexander et al., 2009; Anaclet et al., 2014). Control rats were injected with saline in the pSOM. We targeted these injections to the following coordinates: rat RVM [AP = −10.3 mm, ML = 0 mm, DV = −8.6 mm, 120 nL], rat pSOM [AP = −11.5 mm, ML = 0 mm, DV = −8.4 mm, 120 nL], mouse pSOM [AP = −6.5 mm, ML = 0 mm, DV = −4.8 mm].

For selective deletions of Vgat + GABAergic neurons in the pSOM, Vgat-IRES-Cre mice (n = 5) were injected with Cre dependent AAV-DTA (described above) into the pSOM (AP = −6.5 mm, ML = 0 mm, DV = −4.8 mm; 100 nL). Wildtype littermates receiving similar injections served as controls. For selective activation of Vgat + GABAergic neurons in the pSOM, Vgat-IRES-Cre mice (n = 5) were injected with AAV-DIO-hM3Dq-mcherry (AAV-hM3Dq; Beth Israel Deaconess Medical Center, USA; 75 nL) into the pSOM. For recording sleep-wake, four EEG screw electrodes (Plastics One, USA) were implanted into the skull, bilaterally in the frontal and parietal plates. Two flexible EMG electrodes were implanted into the dorsal neck muscles and the free ends of EMG and EEG electrodes were secured into a socket and attached to the skull with cyanoacrylate glue and dental cement.

4.2.1. EEG/EMG recordings—4 weeks after postoperative recovery, rats were placed into an isolated recording chamber, connected with a recording cable to a commutator, and allowed to habituate for 24 h. For lesions, continuous EEG/EMG and time-locked video was

recorded for 24 h beginning at lights off (1900). For activation and vehicle experiments, i.p. injections of clozapine-n-oxide (CNO, 0.2 mg/kg in rats, 0.3 mg/kg in mice Sigma) or 0.9% saline were made at 1600, 3 h before lights off, with continuous EEG/EMG and time-locked video recorded for 24 h. This injection time was chosen because of the high concentration of REM sleep during this time and to include times of both normally occurring sleep and wakefulness during the typical window of CNO action. The injection order was the same in all animals (saline, CNO). For mice, recordings were begun after 24 h habituation. To focus on REM sleep within the window of CNO action (Alexander et al., 2009), injections were made at 10 AM and recordings were analyzed for 10 h after injection, all during the light period.

To analyze the behavior during REM sleep, video recordings obtained at 30 frames per second were extracted into individual frames using ffmpeg. Subsequently, using a custom script running imagemagick, individual frames were desaturated and compared to subsequent frames to generate a difference frame, with the intensity of each pixel reflecting the change between frames. These difference frames were thresholded to eliminate false-positive difference pixels from video noise. The difference frames were color-coded, made partially transparent, and montaged into a single image to show movement.

The EEG/EMG data from each rat or mouse was digitized at 256 hz and imported into SleepSign (KisseiComtec) and divided into 10 s epochs for rats and 12 s for mice. A bandpass filter was applied to the EEG (0.5–60 hz) and a highpass filter was applied to the EMG (10 hz). EEG/EMG epochs were automatically scored as wake, NREM sleep, or REM sleep using previously defined criteria (Anaclet et al., 2012). Briefly, we first applied automatic scoring in SleepSign that identifies wake, NREM sleep, or REM sleep epochs using parameters derived from the EEG and EMG. specifically, wake epochs are identified based on high-EMG signal, low-amplitude EEG, and lack of delta power. NREM sleep is identified based on low-EMG signal and high-amplitude EEG with abundant delta power (0.5–4.5 hz). REM sleep is identified based on very low-EMG signal, low-amplitude EEG with a high theta (5–10 hz) to delta ratio. The transition from NREM to REM sleep often contains high-theta, high-amplitude EEG with a decline in the integral of the EMG signal; we scored these epochs as NREM sleep based on the amplitude of the EEG. After automatic scoring, all epochs were visually inspected for accuracy. Group differences in total sleep state amounts were tested using the Student's *t*-test, or, in the case of the excitation/inhibition experiments, paired-sample *t*-test comparing the post-CNO recording with the post-saline recording in the same animal.

Parameters from the scored epochs of sleep were used for analysis of EEG and EMG changes. Specifically, for detecting EMG spikes, we calculated the integral of the absolute value of the EMG, as well as the maximum amplitude of the EMG within a given epoch. To determine a baseline EMG, we took the mode of the absolute value maximum amplitude during REM sleep. We then automatically scored the number of times that the absolute EMG signal crosses a threshold of twice this value. To assess EEG changes, we derived the power of the EEG in delta (0.5–4.5 hz), theta (5–10 hz), alpha (10.5–20 hz), and beta/gamma (20–50 hz) frequency bands using a Fast Fourier Transform (FFT). We calculated

the FFT every hour and either averaged over 24 h (lesion experiments) or split data into the 6 h after CNO, the 18 h after the CNO window, and the 24 h total.

4.3. Immunohistochemistry

Animals were perfused within 2 weeks of recording with 10% buffered formalin (Fisher Scientific, Pittsburgh PA) and brains were transferred to a solution of 20% sucrose and PBS containing 0.02% sodium azide overnight, then sliced into four series of 40 μm sections using a freezing microtome. For characterizing lesions, sections were stained with 0.1% Thionin (Sigma, St Louis MO). We stained for YFP or mCherry by incubating tissue in primary polyclonal anti-GFP 1:20,000 (Invitrogen) or rabbit anti-mCherry (1:10,000; Clontech) for 24 h, followed by 1 h incubation in biotinylated secondary antiserum in PBST (Vector Laboratories). We stained for c-Fos by incubating tissue in primary cFos (1:20,000 Ab-5, PC38, rabbit polyclonal, Calbiochem, Billerica, MA) for 48 h, followed by 1 h incubation in biotinylated secondary antiserum in PBST (Vector Laboratories).

After washing with PBS, tissue was incubated with an avidin-biotin-horseradish peroxidase conjugate (Vector laboratories) and stained brown (YFP) with 0.05% 3,3-diaminobenzidine tetrahydrochloride (Sigma, St. Louis MO) and 0.02% H_2O_2, or black (c-Fos) with the addition of 0.05% cobalt chloride and 0.01% nickel ammonium sulfate for double-stained sections showing the presence of both YFP and c-Fos.

Sections were then mounted onto slides, dehydrated, and coverslipped.

Supplementary Material

Refer to Web version on PubMed Central for supplementary material.

Acknowledgments

The authors acknowledge the expert technical assistance of Quan Ha and Xi Chen. This work was funded by the Hilda and Preston Davis Foundation (M.C.C.) and National Institutes of Health (NS088482 to R.V.; NS073613 and NS092652 to P.M.F; NS062727 and NS061841 to J.L.).

References

Alexander GM, Rogan SC, Abbas AI, Armbruster BN, Pei Y, Allen JA, Nonneman RJ, Hartmann J, Moy SS, Nicolelis MA, McNamara JO, Roth BL. Remote control of neuronal activity in transgenic mice expressing evolved G protein-coupled receptors. Neuron. 2009; 63:27–39. [PubMed: 19607790]

Anaclet C, Lin JS, Vetrivelan R, Krenzer M, Vong L, Fuller PM, Lu J. Identification and characterization of a sleep-active cell group in the rostral medullary brainstem. J Neurosci. 2012; 32:17970–17976. [PubMed: 23238713]

Anaclet C, Ferrari L, Bass C, Saper CB, Lu J, Fuller PM. The GABAergic parafacial zone is a medullary slow-wave sleep-promoting center. Nat Neurosci. 2014; 17(9):1217–1224. [PubMed: 25129078]

Boissard R, Gervasoni D, Schmidt MH, Barbagli B, Fort P, Luppi PH. The rat ponto-medullary network responsible for paradoxical sleep onset and maintenance: a combined microinjection and functional neuroanatomical study. Eur J Neurosci. 2002; 16:1959–1973. [PubMed: 12453060]

Brooks PL, Peever JH. Glycinergic and GABAA-mediated inhibition of somatic motoneurons does not mediate rapid eye movement sleep motor atonia. J Neurosci. 2008; 28:3535–3545. [PubMed: 18385312]

Castillo P, Pedroarena C, Chase MH, Morales FR. A medullary inhibitory region for trigeminal motoneurons in the cat. Brain Res. 1991; 549:346–349. [PubMed: 1884229]

Chase MH. Motor control during sleep and wakefulness: clarifying controversies and resolving paradoxes. Sleep Med Rev. 2013; 17:299–312. [PubMed: 23499211]

Chase MH, Morales FR. The atonia and myoclonia of active (REM) sleep. Annu Rev Psychol. 1990; 41:557–584. [PubMed: 1968326]

Chase MH, Enomoto S, Hiraba K, Katoh M, Nakamura Y, Sahara Y, Taira M. Role of medullary reticular neurons in the inhibition of trigeminal motoneurons during active sleep. Exp Neurol. 1984; 84:364–373. [PubMed: 6714349]

Chase MH, Soja PJ, Morales FR. Evidence that glycine mediates the postsynaptic potentials that inhibit lumbar motoneurons during the atonia of active sleep. J Neurosci. 1989; 9:743–751. [PubMed: 2926479]

Drew T, Rossignol S. Functional organization within the medullary reticular formation of intact unanesthetized cat. I. Movements evoked by microstimulation. J Neurophysiol. 1990; 64:767–781. [PubMed: 2230923]

Fort P, Luppi PH, Jouvet M. Glycine-immunoreactive neurones in the cat brain stem reticular formation. Neuroreport. 1993; 4:1123–1126. [PubMed: 8219038]

Fuller PM, Fuller P, Sherman D, Pedersen NP, Saper CB, Lu J. Reassessment of the structural basis of the ascending arousal system. J Comp Neurol. 2011; 519:933–956. [PubMed: 21280045]

Hajnik T, Lai YY, Siegel JM. Atonia-related regions in the rodent pons and medulla. J Neurophysiol. 2000; 84:1942–1948. [PubMed: 11024087]

Holmes CJ, Jones BE. Importance of cholinergic, GABAergic, serotonergic and other neurons in the medial medullary reticular formation for sleep-wake states studied by cytotoxic lesions in the cat. Neuroscience. 1994; 62:1179–1200. [PubMed: 7845593]

Holstege JC, Bongers CM. A glycinergic projection from the ventromedial lower brainstem to spinal motoneurons. An ultrastructural double labeling study in rat. Brain Res. 1991; 566:308–315. [PubMed: 1726063]

Hossaini M, Goos JAC, Kohli SK, Holstege JC. Distribution of glycine/GABA neurons in the ventromedial medulla with descending spinal projections and evidence for an ascending glycine/GABA projection. PLoS One. 2012; 7:e35293. [PubMed: 22558137]

Krenzer M, Anaclet C, Vetrivelan R, Wang N, Vong L, Lowell BB, Fuller PM, Lu J. Brainstem and spinal cord circuitry regulating REM sleep and muscle atonia. PLoS One. 2011; 6:e24998. [PubMed: 22043278]

Lai YY, Siegel JM. Brainstem-mediated locomotion and myoclonic jerks. I. Neural substrates. Brain Res. 1997; 745:257–264. [PubMed: 9037417]

Lai Y-Y, Kodama T, Schenkel E, Siegel JM. Behavioral response and transmitter release during atonia elicited by medial medullary stimulation. J Neurophysiol. 2010; 104:2024–2033. [PubMed: 20668280]

Lu J, Sherman D, Devor M, Saper CB. A putative flip-flop switch for control of REM sleep. Nature. 2006; 441:589–594. [PubMed: 16688184]

Luppi P-H, Gervasoni D, Verret L, Goutagny R, Peyron C, Salvert D, Leger L, Fort P. Paradoxical (REM) sleep genesis: the switch from an aminergic–cholinergic to a GABAergic–glutamatergic hypothesis. J Physiol Paris. 2006; 100:271–283. [PubMed: 17689057]

Martin EM, Pavlides C, Pfaff D. Multimodal sensory responses of nucleus reticularis gigantocellularis and the responses' relation to cortical and motor activation. J Neurophysiol. 2010; 103:2326–2338. [PubMed: 20181730]

Martin, Em, Devidze, N., Shelley, Dn, Westberg, L., Fontaine, C., Pfaff, Dw. Molecular and neuroanatomical characterization of single neurons in the mouse medullary gigantocellular reticular nucleus. J Comp Neurol. 2011; 519:2574–2593. [PubMed: 21456014]

Morales FR, Sampogna S, Yamuy J, Chase MH. c-Fos expression in brainstem premotor interneurons during cholinergically induced active sleep in the cat. J Neurosci. 1999; 19:9508–9518. [PubMed: 10531453]

Morrison JL, Sood S, Liu H, Park E, Liu X, Nolan P, Horner RL. Role of inhibitory amino acids in control of hypoglossal motor outflow to genioglossus muscle in naturally sleeping rats. J Physiol. 2003; 552:975–991. [PubMed: 12937280]

Nakamura Y, Goldberg LJ, Chandler SH, Chase MH. Intracellular analysis of trigeminal motoneuron activity during sleep in the cat. Science. 1978; 199:204–207. [PubMed: 202025]

Stornetta RL, Guyenet PG. Distribution of glutamic acid decarboxylase mRNA-containing neurons in rat medulla projecting to thoracic spinal cord in relation to monoaminergic brainstem neurons. J Comp Neurol. 1999; 407:367–380. [PubMed: 10320217]

Takakusaki K, Kohyama J, Matsuyama K, Mori S. Medullary reticulospinal tract mediating the generalized motor inhibition in cats: parallel inhibitory mechanisms acting on motoneurons and on interneuronal transmission in reflex pathways. Neuroscience. 2001; 103:511–527. [PubMed: 11246165]

Vetrivelan R, Fuller PM, Tong Q, Lu J. Medullary circuitry regulating rapid eye movement sleep and motor atonia. J Neurosci. 2009; 29:9361–9369. [PubMed: 19625526]

Vong L, Ye C, Yang Z, Choi B, Chua S Jr, Lowell BB. Leptin action on GABAergic neurons prevents obesity and reduces inhibitory tone to POMC neurons. Neuron. 2011; 71:142–154. [PubMed: 21745644]

Weber F, Chung S, Beier KT, Xu M, Luo L, Dan Y. Control of REM sleep by ventral medulla GABAergic neurons. Nature (advance online publication). 2015

Weng, Fj, Williams, Rh, Hawryluk, Jm, Lu, J., Scammell, Te, Saper, Cb, Arrigoni, E. Carbachol excites sublaterodorsal nucleus neurons projecting to the spinal cord. J Physiol. 2014; 492:1601–1617.

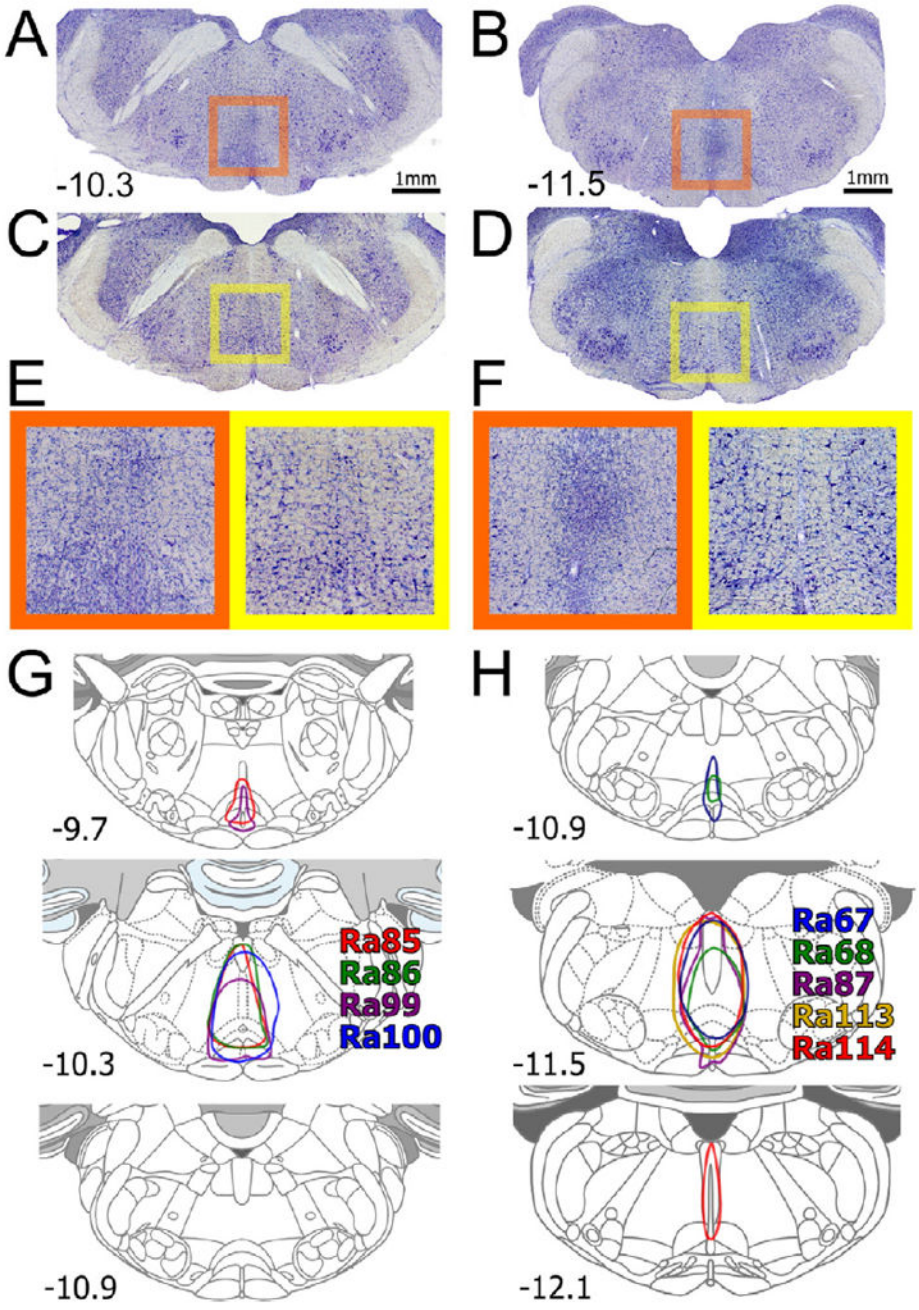

Fig. 1.

Injection of AAV-DTA into the RVM (A) and pSOM (B) of the rat medulla results in near complete cell loss along the midline, whereas injections of saline into the RVM (C) and pSOM (D) do not. High-magnification images of the insets (E–F) show cell loss in the lesion areas (left panels) compared to cell preservation in the saline injections (right panels). Overlay of lesion center of mass is shown at the multiple levels (G–H).

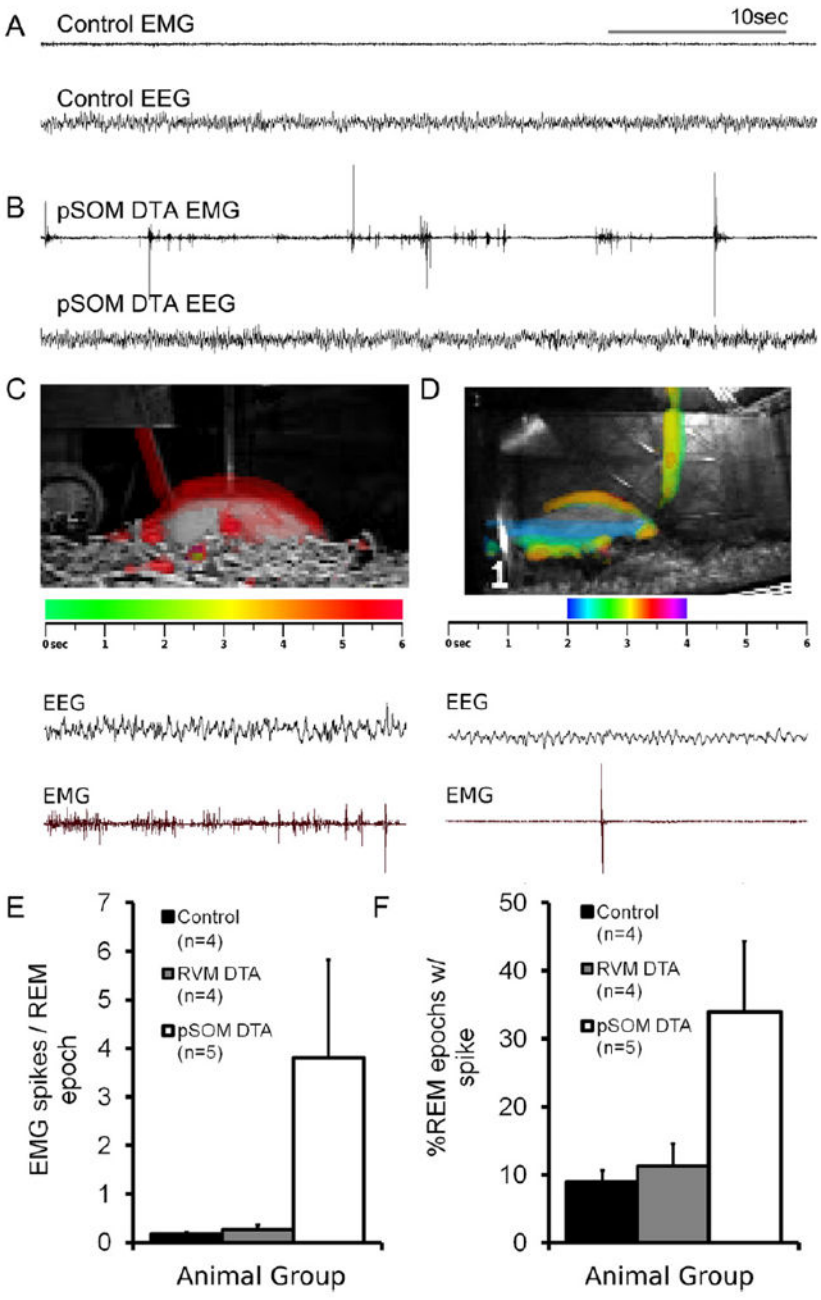

Fig. 2.

Lesions of the pSOM result in EMG and behavior during REM sleep. Control animals have a flat, monotonous EMG during REM sleep (A), while pSOM DTA animals have numerous EMG spikes during REM sleep (B). Color-coded video analysis of movement (C–D) shows body movements overlaid as colors over a black and white still image. The colored regions show the extent of the body movements, with a color bar legend overlaid with a timescale to show when the movement–and corresponding color–occurred, relative to the EEG and EMG; e.g. in Panel C, the red-colored movements overlaid on the video occurred 5 s into the

presented EEG/EMG data (C). Panel D shows a series of myoclonic twitches during REM sleep, in which multiple movements, colored blue to green to orange, occur from 2 to 3.5 s into the presented EEG/EMG data (D). pSOM lesioned animals, but not RVM lesioned animals, have significant increases in EMG spikes per REM epoch (E) and the percentage of REM epochs containing at least one EMG spike (F). Data are represented as mean ± SEM.

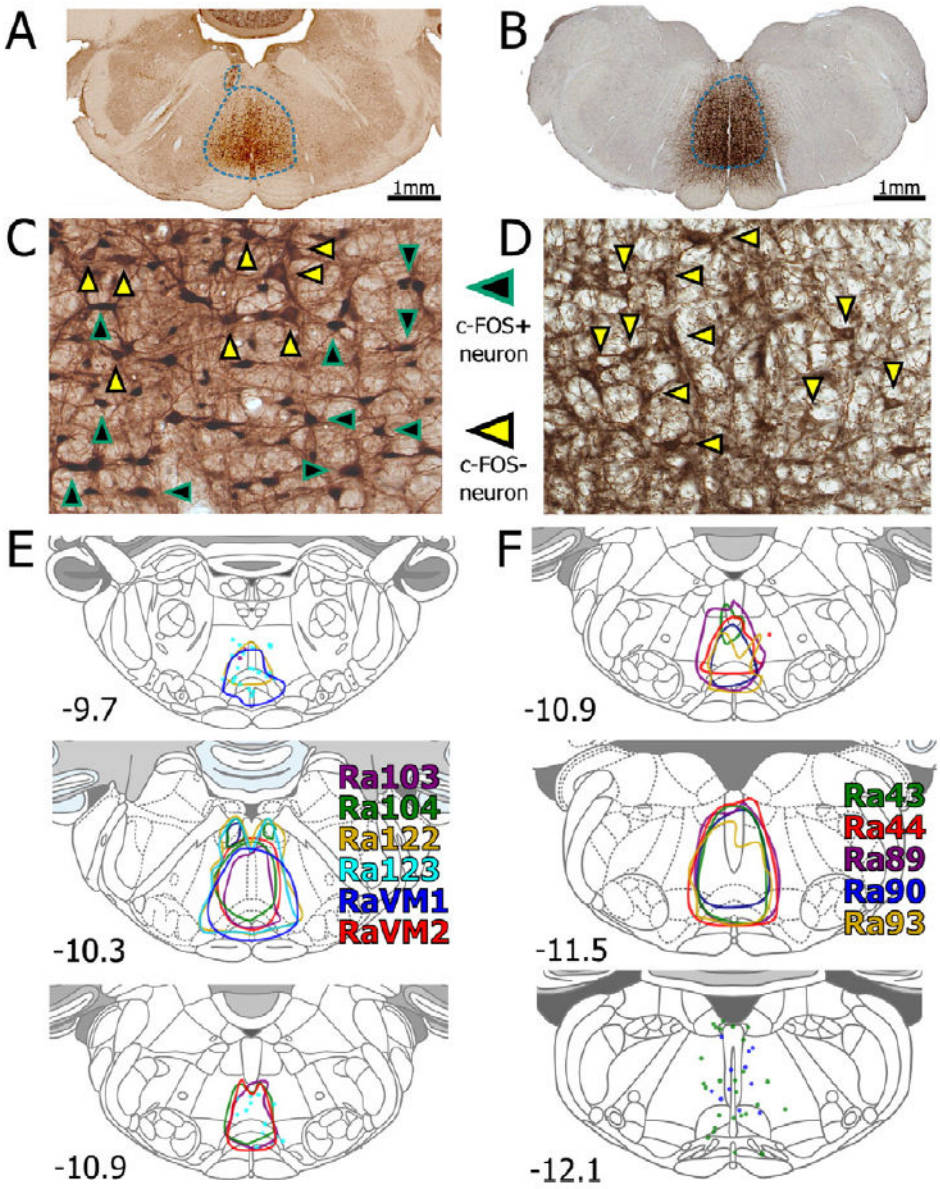

Fig. 3.

Injection site of an AAV mixture into the RVM (A) and pSOM (B) regions are delimited by a DAB-based stain against mCherry. Following CNO injections (IP, 0.2 mg/kg), most transduced cells within the RVM or pSOM sites expressed c-Fos, demonstrating strong cellular activation by CNO (C). After CNO injection, both c-Fos positive double-stained neurons (black/teal arrows) are visible, as well as c-Fos negative, non-double-stained neurons (yellow-black arrows). In contrast, saline injections did not elicit c-Fos expression in transduced ventromedial medulla neurons (D), with no double-staining (yellow-black arrows). Overlays of the center of RVM injections (E) and pSOM injections (F) at multiple levels show the extent of the transduced area, with sporadic neurons in more caudal sections (colored dots).

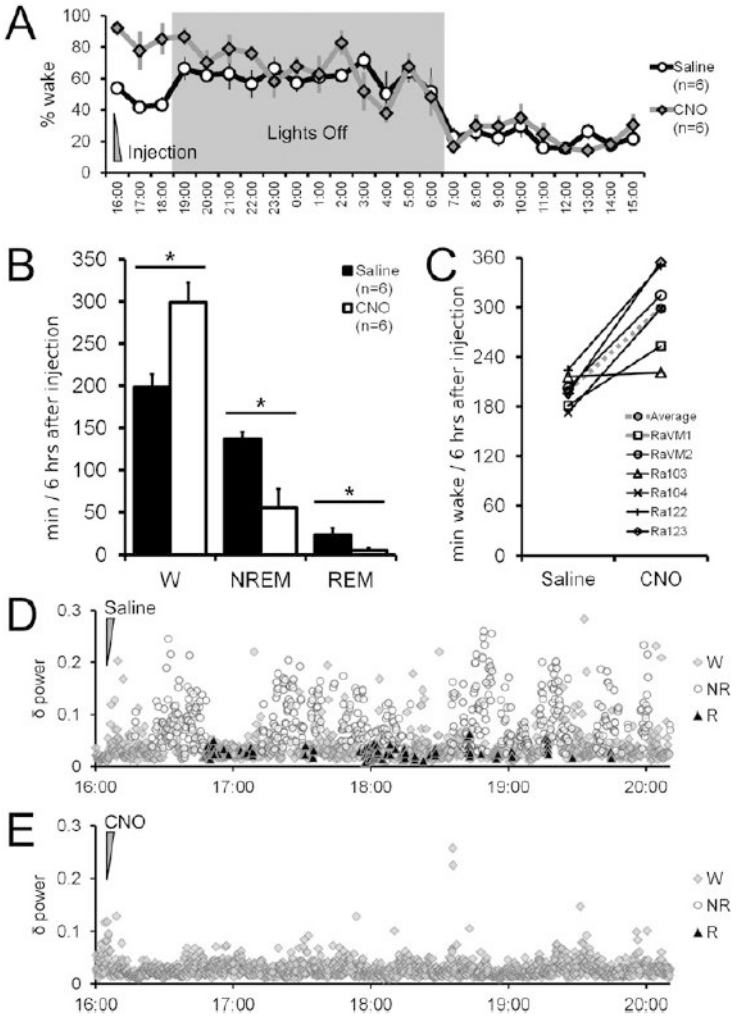

Fig. 4.

Injection (IP; 0.2 mg/kg) of CNO activates RVM neurons and increases wakefulness for several hours (A). Over the 6 h period of highest CNO effect, RVM virus animals have significantly higher wakefulness and lower NREM and REM sleep after CNO injection than after saline injection (B). Each animal experienced an increase in wakefulness in the 6 h following CNO injection compared to the same time period following saline injection (C). An example 4-hour hypnogram is shown for a single animal after injection with saline (D) or CNO (E). FFT delta power, a marker of NREM sleep, is plotted against time, with scored stages shown. Saline-injected animals alternated between wake, NREM, and REM sleep, while CNO-injected animals fail to initiate NREM or REM sleep episodes and exhibited low delta power.

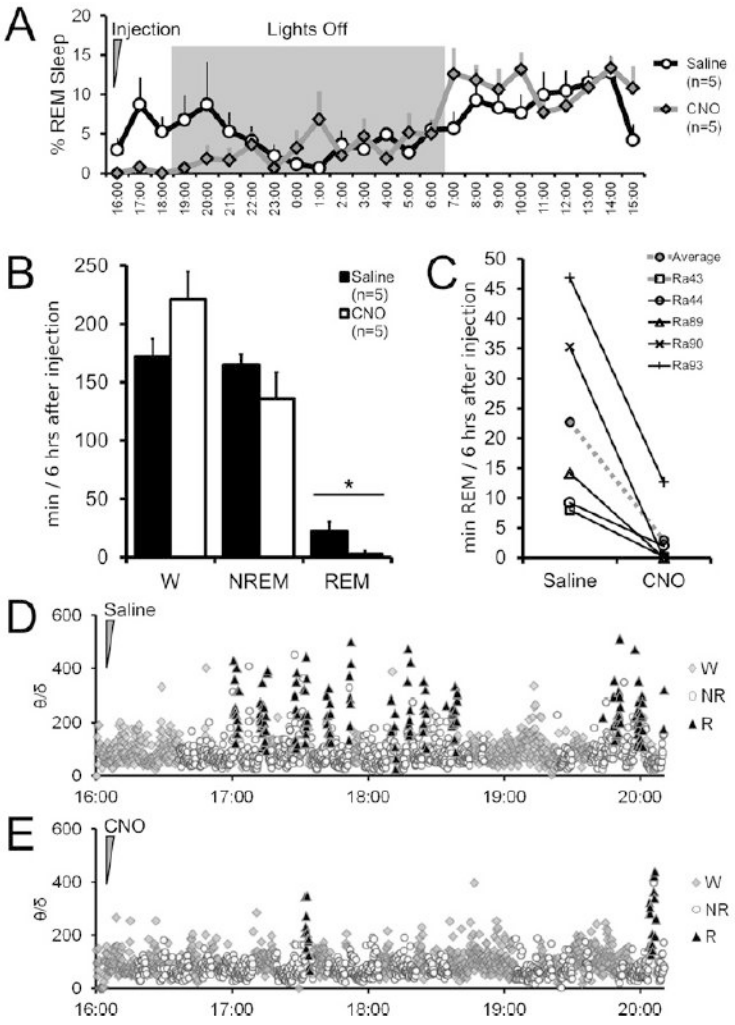

Fig. 5.

Injection (IP; 0.2 mg/kg) of CNO activated pSOM neurons and resulted in a reduction of REM sleep that lasted approximately 6 h (A). Following the REM suppression, total REM sleep time normalizes within a 24 h period, suggesting homeostatic regulation following CNO washout. Over the 6 h period of highest CNO effect, pSOM virus animals have significantly lower REM sleep after CNO injection than after saline injection (B), with no significant changes in wake or NREM sleep. Each animal experienced a steep decline in REM sleep in the 6 h following CNO injection compared to the same time period following saline injection (C). An example 4-hour hypnogram is shown for a single animal after injection with saline (D) or CNO (E). The theta/delta ratio, one marker of REM sleep, is plotted against time, with scored stages shown. Saline-injected animals alternate between wake, NREM, and REM sleep, while CNO-injected animals failed to initiate REM sleep episodes but continued to cycle between wake and NREM sleep.

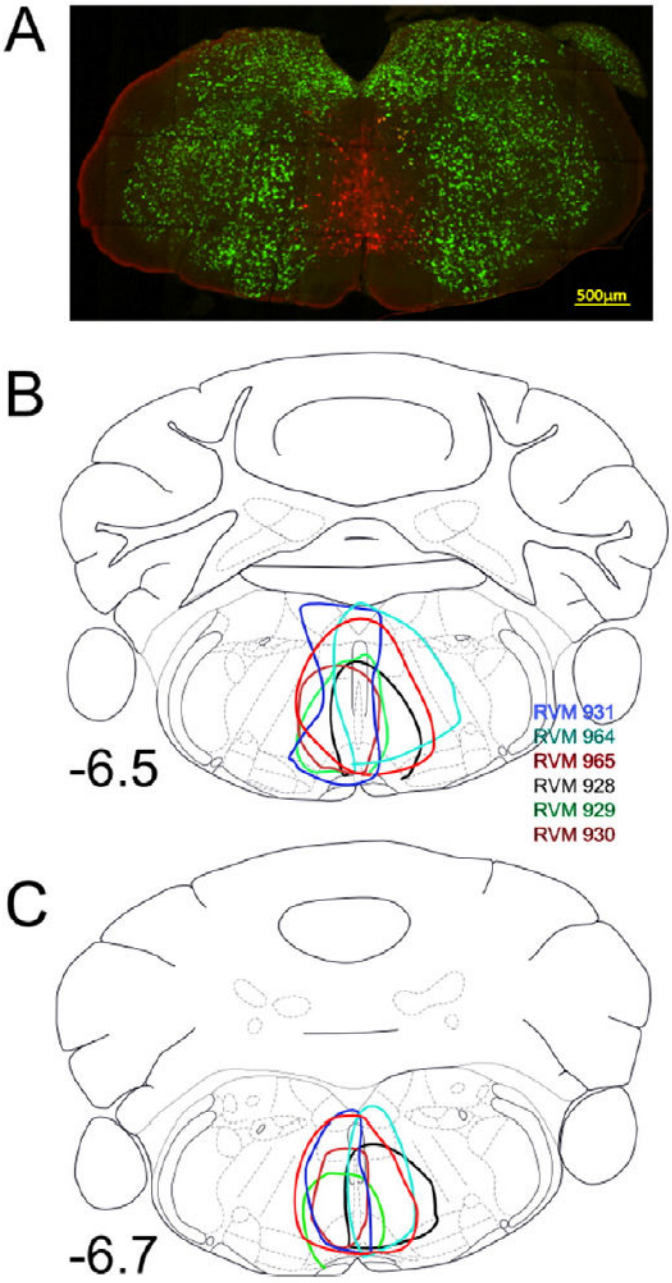

Fig. 6.

Injection of AAV-DTA into the pSOM level of Vgat-IRES-cre mice (A). In Vgat-IRES-cre mice, VGAT neurons express GFP; while AAV-DTA transduced neurons express dsRed. Injections in the pSOM result in complete loss of GFP+ VGAT neurons, while sparing non-GABA/glycine neurons in the same region. Overlay of lesion center of mass is shown at the multiple levels (B–C).

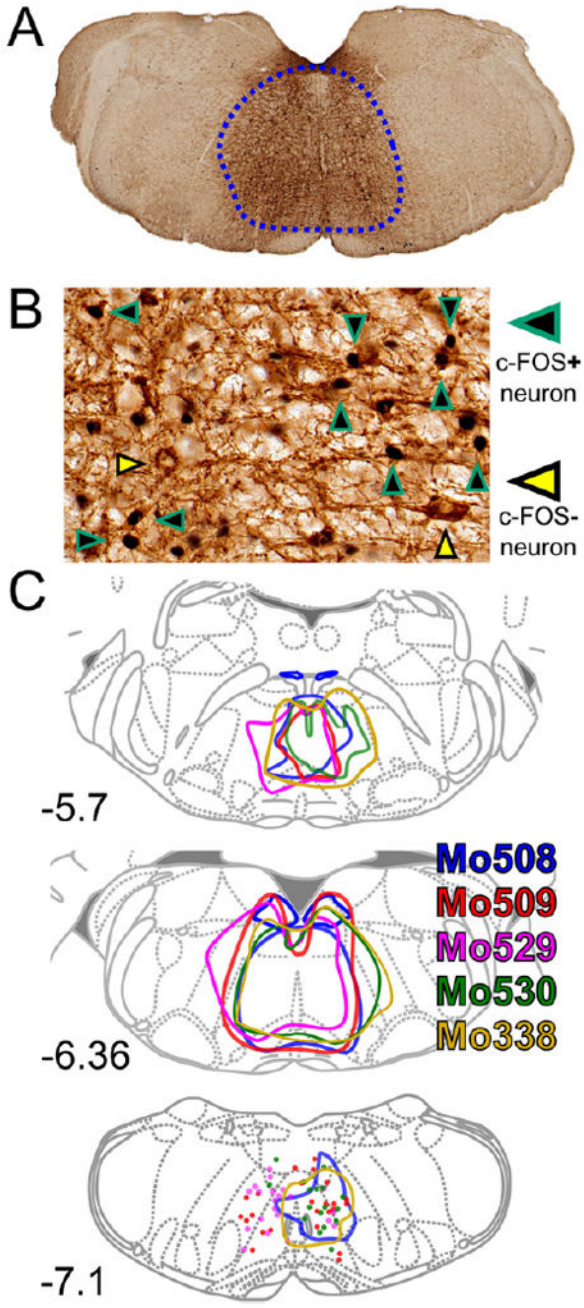

Fig. 7.

Injection of an AAV mixture into the pSOM level of Vgat-IRES-cre mice are delimited by a DAB-based stain against mCherry (A). Administration of CNO (IP, 0.3 mg/kg) produced c-Fos expression in most cells, demonstrating strong cellular activation (B). Overlays of the center of injection mass at the pSOM level and adjoining levels (C) show the extent of the transduced area, with sporadic neurons in more caudal sections (colored dots).

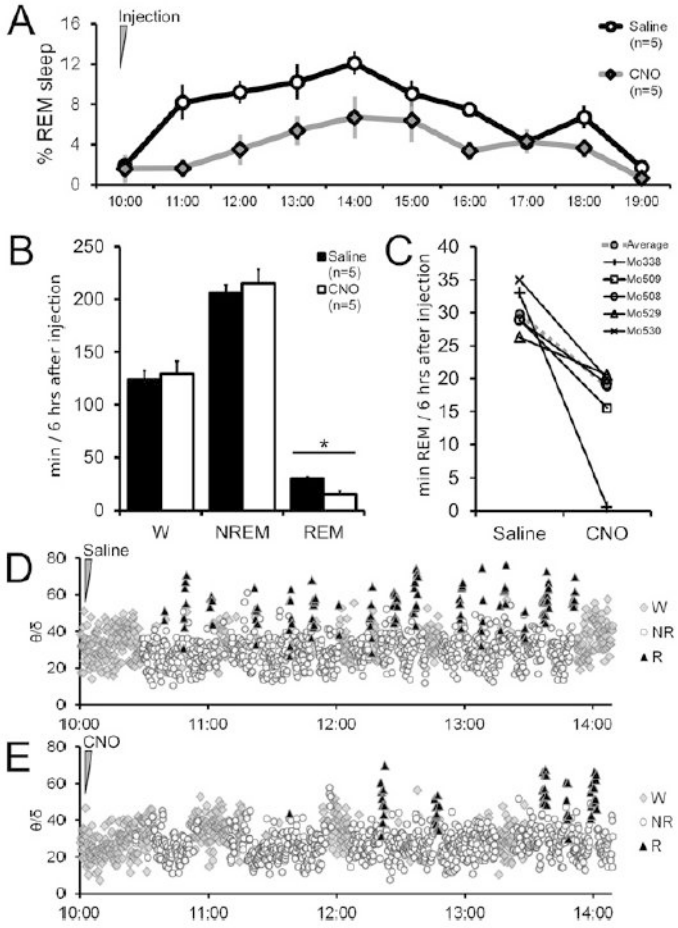

Fig. 8.

CNO activation of glycine/GABA neurons in the pSOM suppressed REM sleep. After injection with CNO, Vgat-cre mice experience a reduction of REM sleep lasting 6 h, similar to rats (A). Over the first 6 h after CNO injection, mice have reduced REM but no changes in wake or NREM sleep compared to the same period after saline injection. Each mouse experienced a decline in REM sleep time over 6 h after CNO injection compared to after saline injection. An example 3-hour hypnogram is shown for a single animal after injection with saline (D) or CNO (E). The theta/delta ratio, one marker of REM sleep, is plotted against time, with scored stages shown. Saline-injected animals alternate between wake, NREM, and REM sleep, while CNO-injected animals fail to initiate REM sleep episodes but continue to cycle between wake and NREM sleep.